PAPER

Development of metastatic brain disease involves progression through lung metastases in *EGFR* mutated non-small cell lung cancer

Convergent Science Physical Oncology

PAPER

Development of metastatic brain disease involves progression through lung metastases in *EGFR* mutated non-small cell lung cancer

RECEIVED
13 December 2016

REVISED
2 June 2017

ACCEPTED FOR PUBLICATION
20 June 2017

PUBLISHED
13 July 2017

Gino K. In[1], Jeremy Mason[2], Sonia Lin[1], Paul K Newton[1,3], Peter Kuhn[1,2,3,4] and Jorge Nieva[1]

[1] Norris Comprehensive Cancer Center, Keck School of Medicine, Division of Oncology, University of Southern California, 1441 Eastlake Ave, NOR 3444, Los Angeles, CA 90033, United States of America
[2] Department of Biological Sciences, Dornsife College of Letters, Arts, and Sciences, University of Southern California, 3616 Trousdale Pkwy, Los Angeles, CA 90089, United States of America
[3] Department of Aerospace and Mechanical Engineering, Viterbi School of Engineering, University of Southern California, 3650 McClintock Ave, Los Angeles, CA 90089, United States of America
[4] Department of Biomedical Engineering, Viterbi School of Engineering, University of Southern California, 3650 McClintock Ave, Los Angeles, CA 90089, United States of America

E-mail: gino.in@med.usc.edu (Gino K. In), masonj@usc.edu (Jeremy Mason), sonia.lin@med.usc.edu (Sonia Lin), newton@usc.edu (Paul K Newton), pkuhn@usc.edu (Peter Kuhn) and jorge.nieva@med.usc.edu (Jorge Nieva)

Keywords: non small cell lung cancer, epidermal growth factor receptor, brain metastases, Markov modeling, EGFR, NSCLC, lung metastases

Supplementary material for this article is available online

Abstract

Lung cancer is often classified by the presence of oncogenic drivers, such as epidermal growth factor receptor (EGFR), rather than patterns of anatomical distribution. While metastatic spread may seem a random and unpredictable process, we explored the possibility of using its quantifiable nature as a measure of describing and comparing different subsets of disease. We constructed a database of 664 non-small cell lung cancer (NSCLC) patients treated at the University of Southern California Norris Comprehensive Cancer Center and the Los Angeles County Medical Center. Markov mathematical modeling was employed to assess metastatic sites in a spatiotemporal manner through every time point in progression of disease. Our findings identified a preferential pattern of primary lung disease progressing through lung metastases to the brain amongst EGFR mutated ($EGFR^m$) NSCLC patients, with exon 19 deletions or exon 21 L858R mutations, as compared to EGFR wild type ($EGFR^{wt}$). The brain was classified as an anatomic 'sponge', with a higher ratio of incoming to outgoing spread, for $EGFR^m$ NSCLC. Bone metastases were more commonly identified in $EGFR^{wt}$ patients. Our study supports a link between the anatomical and molecular characterization of metastatic lung cancer. Improved understanding of the differential biology that drives discordant patterns of anatomic spread, based on genotype specific profiling, has the potential to improve personalized oncologic care.

Introduction

Metastatic spread in lung cancer typically involves the contralateral lung, liver, bone, brain and lymph nodes. This is a seemingly random process, which has not yet been well quantified. Rather than defining lung cancer by its pattern of anatomical distribution, subsets of this disease are more commonly defined by oncogenic drivers such as EGFR (epidermal growth factor receptor), ALK (anaplastic lymphoma kinase), and ROS1 (ROS1 proto-oncogene receptor tyrosine kinase). These driver mutations are both clinically predictive and prognostic, as these subtypes respond to targeted therapeutic agents [1–3].

When comparing primary EGFR mutated ($EGFR^m$) lung cancer, including exon 19 deletions and exon 21 L858R mutations, with EGFR wild type ($EGFR^{wt}$) lung cancer, these subtypes have been anecdotally reported to differ in their anatomic patterns of local progression [4–7]. Tseng *et al* [8] noted that primary $EGFR^m$ lung cancers occur more frequently in the upper lobe compared to $EGFR^{wt}$, while Enomoto *et al* [5] reported that primary $EGFR^m$ tumors had significantly lower nodal stage compared to wild type. Studies have also

suggested distinct metastatic profiles when comparing $EGFR^m$ with $EGFR^{wt}$ lung cancer. Among patients with locally advanced disease treated with chemoradiation, $EGFR^m$ tumors recur with distant metastases more often than wild type [9, 10]. In addition, at least two studies found that the brain was the most common site of distant metastases for $EGFR^m$ tumors [9, 11].

A number of studies have suggested a predilection of $EGFR^m$ lung cancer to spread towards the bone [12], lung [5, 13–16], liver [4], and brain [12, 17, 18]. Hasegawa *et al* [13] described an increased frequency of bilateral lung metastases among patients with $EGFR^m$ lung tumors. Wu *et al* [19] reported that the presence of liver metastases was associated with bone metastases as well as a trend towards lung metastases. Additional studies suggest that anatomical differences in metastatic spread exist between exon 19 deleted and exon 21 mutated $EGFR^m$ tumors as well [8, 20].

Of particular interest to the authors is the evidence that $EGFR^m$ non-small cell lung cancer (NSCLC) prefers the brain as a metastatic site. The percentage of $EGFR^m$ lung cancer patients who present with brain metastases at diagnosis has been estimated at 15.7–49% [6, 7, 9, 11, 12, 15, 16, 18, 21–25]. Rangachari *et al* [7] reported the percentage of patients with $EGFR^m$ lung cancer who develop brain metastases increases from 24% at diagnosis up to 52.9% by 5 years. Sekine *et al* [26] demonstrated that $EGFR^m$ lung cancer patients tended to have a significantly higher number of synchronous brain metastases at diagnosis compared to $EGFR^{wt}$ patients. It remains unclear why patients with $EGFR^m$ lung cancers display increased brain metastases. These patients clearly live longer and as such, have a higher lifetime risk, but whether there is also a different causative biology remains to be determined.

Markov modeling is a probability based method that can be used to model randomly changing systems, and thus may provide a more accurate means for assessing patterns of metastatic cancer spread [27]. These models function under the assumption that future events occur independently of past events, and only consider the current state of the system. This approach is useful for complex decision problems such as metastatic cancer, where risk of metastatic events is continuous over time, metastatic events may occur more than once, and the timing of these events has distinct clinical outcomes [28].

In this study, we constructed a database of NSCLC patients compiled from the University of Southern California Norris Comprehensive Cancer Center (NCCC) and the Los Angeles County Medical Center (LAC). We utilized Markov modeling to assess metastatic patterns from time of diagnosis throughout treatment history, but also the anatomic pathways by which metastases disseminate. For all patients, we evaluated each anatomic metastatic site at every time point of disease progression. Using this strategy, we quantified the likelihood of top metastatic pathways and conducted Monte Carlo computer simulations as a model for cancer progression. Stochastic modeling was used to simulate metastatic spread by means of random walk processes on directed graphs. Employing the forecasting model of Newton *et al* [27], we characterized metastatic sites as 'spreaders' and 'sponges' based on their ratio of outgoing to incoming probability of spread. We then assessed for differences, using these methodologies, specifically between patients with $EGFR^{wt}$ and $EGFR^m$ NSCLC.

Materials and methods

This retrospective study was approved by the University of Southern California Institutional Review Board, which waived the need for informed consent, given the anonymity of all patients and non-invasive nature of this study.

Database

A retrospective database of patients treated at both NCCC and LAC was created using a tumor registry of patients with NSCLC diagnosis between the years 2005-2015. Among 548 charts at NCCC, and 820 charts at LAC, 262 patients and 402 patients, respectively, met eligibility criteria and were included for analysis, totaling 664 NSCLC patients. Among these patients, well characterized EGFR mutation testing for exon 19 deletions or exon 21 L858R mutations, was available for 161 (24.3%) patients and is included in this analysis. The database also included patient characteristics such as age, gender, smoking history, past medical history, histology, performance status, clinical/surgical staging, treatment history (including surgery, radiation and systemic therapy), use of clinical trials and metastatic sites at each time point of progression. In total, 23 anatomical sites (see legend in figure 3) were included for analysis as metastatic sites.

Eligibility criteria

Inclusion criteria required a confirmed pathological diagnosis of NSCLC at either NCCC or LAC. NSCLC histology subtypes included were: adenocarcinoma, squamous cell, large cell, mixed, or not otherwise specified. Patients with small cell lung cancer, a second/concomitant malignancy within the last 5 years (excluding superficial basal cell cancer or squamous cell skin cancer that was treated by excision alone), or cancer of unknown primary were excluded from the study. In addition, patients who were immediately placed on hospice at diagnosis, who immediately died at diagnosis, or with insufficient follow-up (only initial visit) were excluded. Among those included, metastatic sites were documented from diagnosis and at every time of clinical progression. Patients with documented EGFR mutation testing that showed exon 19 deletions or exon 21 L858R mutations, or EGFR wild type were included in this analysis; patients with no testing, insufficient tissue or unknown EGFR status were excluded.

Radiographic analysis

Metastatic sites were documented based on specific radiographic or histologic criteria consistent with RECIST criteria [29]. Lesions documented by tissue biopsy and hypermetabolic lesions as seen on PET were included. Pleural effusions were included if either documented by cytology from thoracentesis, hypermetabolic based on PET, symptomatic or clinically responsive to treatment. Lung nodules located in a contralateral lobe and pleural nodules were documented as metastatic lung lesions separate from lung primary. Bone metastases, as detected unequivocally by bone scan with increased uptake, sclerotic appearance or multiple lesions, were included. Lesions less than 1 cm in diameter were not included as a metastatic site, unless they were symptomatic, hypermetabolic or grew with progression of disease.

Markov mathematical modeling

Based on the database of lung cancer patients compiled from NCCC and LAC, we evaluated every time point of disease progression, starting at diagnosis, by means of a Markov chain model. The Markov model makes the simple assumption that progression from one state to the next occurs as a random walk on a weighted network with no history dependence, other than the fact that the tumor originated in the lung. This is ideal for our analysis because we are not required to define specific biomechanical, biochemical, or genetic reasons for metastatic spread. Rather, all of this information is encoded in the transition probabilities between each of the states in our model, thus defining the dynamics of how random walkers traverse the network.

Using this method, we assessed metastatic patterns as they evolved over time and quantified major pathways that emerged from Monte Carlo simulations of cancer progression. This type of data is best visualized as a circular tree ring diagram, starting from the center and expanding outwards. In doing so, we demonstrate the spatiotemporal progression of lung cancer, as it disseminates through multiple anatomic sites of metastases over time. We subsequently created reduced models which further illustrate the two most important steps of progression from primary site to distant metastatic site. For each metastatic site, we compared the probability of incoming spread to the probability of outgoing spread. Those sites with a higher incoming probability were classified as 'sponges', while those with higher outgoing probability were classified as 'spreaders'.

Results

NSCLC with EGFR mutations

EGFR mutations, either exon 19 deletion or exon 21 L858R mutations, were documented in a total of 62 patients (9.3%), while 99 patients had $EGFR^{wt}$ and the remaining 503 patients either had insufficient tissue, were not tested, or had unknown status. Given that standardized EGFR profiling began at our institution circa 2011, those patients with EGFR testing performed represent a more recent cohort from our database. $EGFR^{m}$ NSCLC patients showed a significantly higher percentage of Asians, and significantly lower average smoking history, when compared to $EGFR^{wt}$ (table 1). They were also more likely to have more than four lines of therapy, and longer survival. Table 1 highlights additional demographics between the two groups.

Table 1. Patient demographics between $EGFR^{m}$ and $EGFR^{wt}$ NSCLC.

	$EGFR^{m}$ ($n = 62$)	$EGFR^{wt}$ ($n = 99$)	
Median age	60	62	$p = 0.31$
Gender			
Female	43 (69.4%)	59 (59.6%)	$p = 0.23$
Male	19 (30.6%)	40 (40.4%)	$p = 0.20$
Ethnicity			
Asian	34 (54.8%)	25 (25.3%)	$p = 0.0002$
Black	1 (1.6%)	8 (8.1%)	$p = 0.08$
Hispanic	15 (24.2%)	26 (26.3%)	$p = 0.78$
Non-hispanic white	12 (19.4%)	33 (33.3%)	$p = 0.05$
Other	0 (0%)	7 (7.1%)	$p = 0.03$
Smoking			
Average packs year	6.0	21.2	$p = 0.0001$
ECOG			
0	29 (46.8%)	40 (40.4%)	$p = 0.43$
1	32 (51.6%)	52 (52.5%)	$p = 0.91$
2	1 (1.6%)	6 (6.1%)	$p = 0.18$
3	0 (0%)	0 (0.0%)	N/A
4	0 (0%)	1 (1.0%)	$p = 0.43$
Stage			
I	6 (9.7%)	5 (5.1%)	$p = 0.26$
II	0 (0.0%)	8 (8.1%)	$p = 0.02$
III	11 (17.7%)	14 (14.1%)	$p = 0.54$
IV	45 (72.6%)	72 (72.7%)	$p = 0.99$
Lines of therapy			
1	59 (95.2%)	83 (83.8%)	$p = 0.03$
2	42 (67.7%)	52 (52.5%)	$p = 0.06$
3	22 (35.5%)	25 (25.3%)	$p = 0.17$
4	16 (25.8%)	9 (9.1%)	$p = 0.005$
5+	8 (12.9%)	3 (3.0%)	$p = 0.02$
EGFR-targeted therapy	50 (80.6%)	21 (21.2%)	$p < 0.0001$

Survival analysis

Overall survival was estimated from the date of diagnosis to the date of death/hospice or date of last follow up (August 3, 2015). Based on Gehan–Breslow–Wilcoxon testing, $EGFR^{m}$ NSCLC patients had significantly longer overall survival compared to $EGFR^{wt}$ ($p = 0.0005$). Survival curves appear in figure 1.

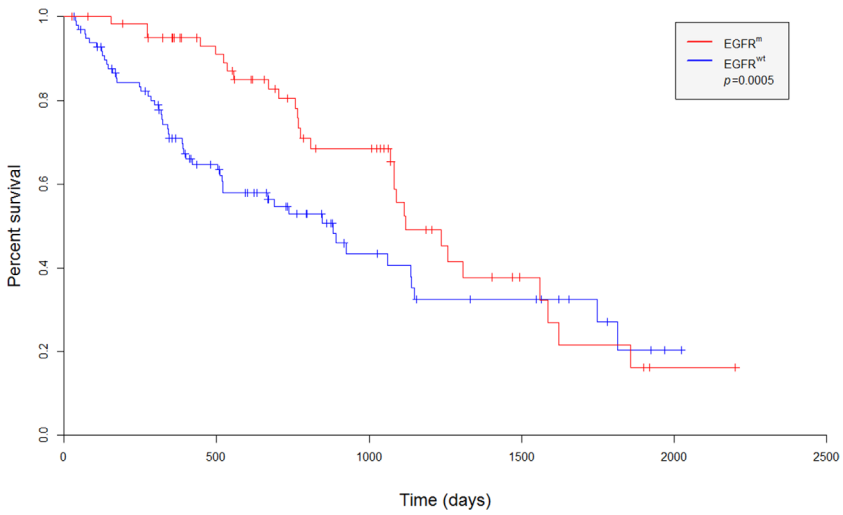

Figure 1. Kaplan–Meier curves depict survival of NSCLC patients with EGFR^{m} and EGFR^{wt} tumors (all stages).

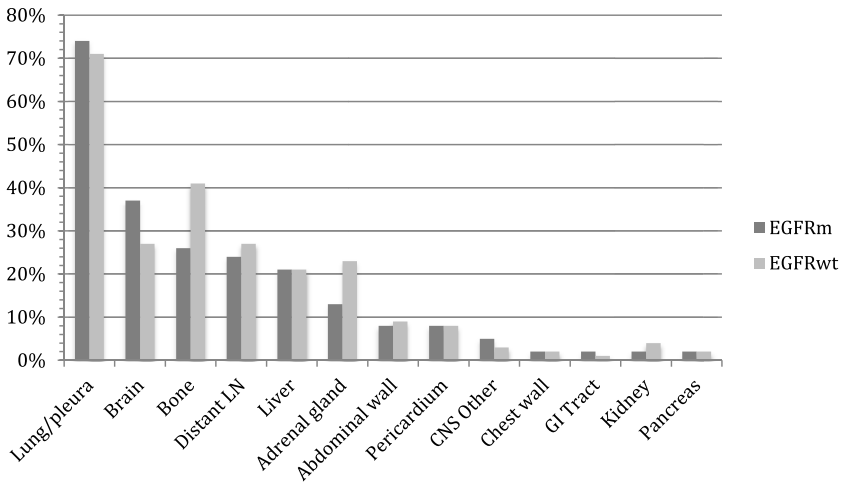

Figure 2. Histogram showing the frequency of most common metastatic sites among non-small cell lung cancer patients with EGFR mutations and EGFR wild type.

Metastatic sites for EGFR^{m} and EGFR^{wt} NSCLC

Metastatic sites were tracked among all patients for up to 7 lines of therapy. Figure 2 displays the percentage of patients who presented with a metastatic site at any time throughout clinical progression. Among EGFR^{m} NSCLC patients, the most frequent metastatic sites were lung/pleura (occurring in 74% of patients), brain (37%), bone (26%), distant lymph nodes (24%), liver (21%), and adrenal gland (13%). Among the EGFR^{wt} group, the most frequent metastatic sites were lung/pleura (72%), bone (41%), brain (27%), distant lymph nodes (27%), adrenal gland (23%), and liver (21%).

Spatiotemporal progression

From the subsets of EGFR^{m} and EGFR^{wt} lung cancer patients, we created spatiotemporal diagrams spanning a 5 year period to illustrate the progression patterns of metastases. Figure 3 demonstrates the metastatic landscape at 5 years after diagnosis and throughout progression of disease. Progression patterns are depicted from the innermost ring (primary lung in gold), to the outermost ring. Each subsequent ring represents a metastatic site and is color-coded accordingly (see legend in figure 3). The circular arc length of a sector represents the percentage of patients with each metastatic site involved, taking into account the previous progression steps.

The tree ring diagrams depict a more preferential spread to the brain in EGFR^{m} patients as compared to EGFR^{wt}. Direct lung → brain metastases occurred with a probability of 12.9% versus 11.1% for EGFR^{m} and EGFR^{wt} NSCLC respectively. Lung primary → lung metastases → brain metastases occurred with a probability of 16.1% versus 10.1% for EGFR^{m} and EGFR^{wt} patients, respectively. Progression from lung metastases → brain metastases as three and four step pathways also occurred with higher frequency amongst EGFR^{m} NSCLC, compared to EGFR^{wt} NSCLC. In contrast, the lung primary → lung metastases → bone metastases occurred with higher probability, 16.2% versus 6.5% for the EGFR^{wt} group, compared to EGFR^{m} NSCLC. All probabilities are listed in table 2.

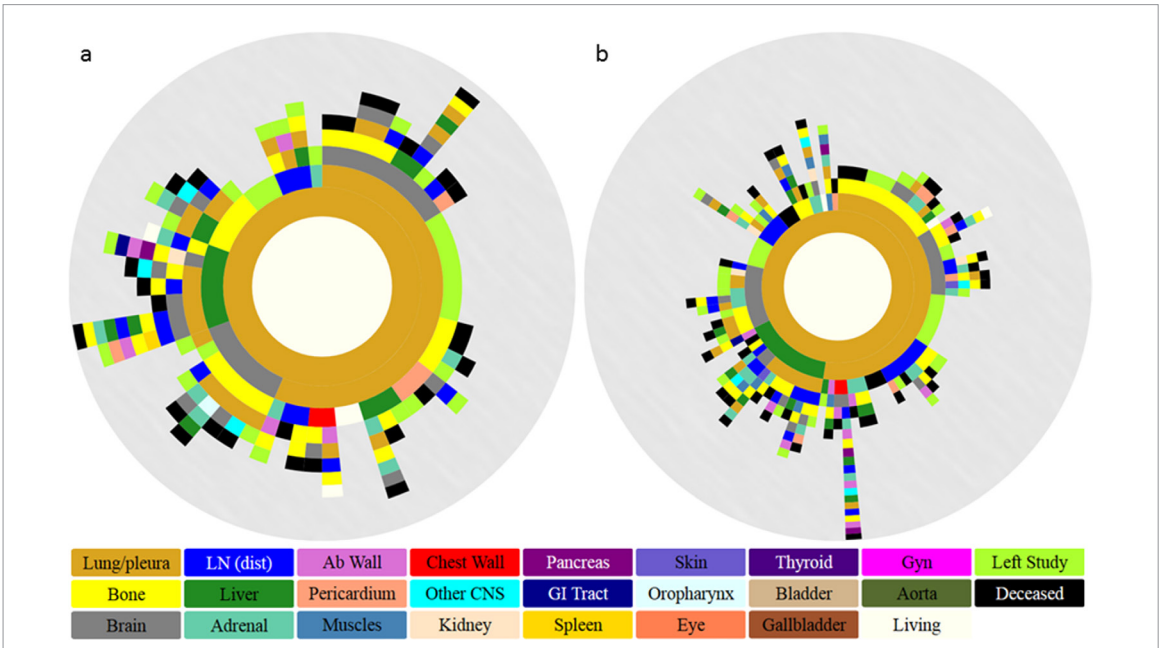

Figure 3. Spatiotemporal progression diagrams over a 5 year period for (a) $EGFR^{m}$ and (b) $EGFR^{wt}$ lung cancer. Innermost to outermost ring illustrates progression patterns from primary lung (inner golden ring) through formation of metastases (subsequent rings). The circular arc length of each ring represents the percentage of patients that progressed to that particular metastasis.

Markov chain networks were used to demonstrate the subsequent dynamics of metastatic progression (figure 4). Transition probability values were calculated and used to arrange metastatic sites clockwise in decreasing order from the primary (located at 12:00 position). The brain was the 2nd most probable (14.3% transition probability) metastatic site for $EGFR^{m}$ NSCLC, while it was the 4th most probable (9.8%) metastatic site for $EGFR^{wt}$ NSCLC. We also show deceased as a site and list it in the last position regardless of how probable it is. The width of each chord at its base represents the one-step transition probability from that site to its respective ending location. It is noted that for the $EGFR^{m}$ network, the brain has transition probabilities to every other metastatic site (deceased included), while in the $EGFR^{wt}$ network, there are only transitions to 10 of the remaining 15 sites.

Metastatic sites as spreaders or sponges

All two-step pathways emanating from the lung were calculated and subsequently rank ordered. We calculate one of these paths as the product of two distinct, one-step transition probabilities (i.e.—Lung → Site A and Site A → Site B). Reduced Markov networks were then created using the top 30 of these pathways emanating from the lung (figure 5). These 30 two-step pathways represent ~88% of all two-step pathways for $EGFR^{m}$ (61 total pathways) and $EGFR^{wt}$ (62 total) patients. The metastatic sites depicted in these diagrams were used to compute the probability of spread for incoming routes (P_{in}) and outgoing routes (P_{out}). Sites were classified as spreaders (shown in red and defined as $P_{out} > P_{in}$) or sponges (shown in blue and defined as $P_{out} < P_{in}$) based on their pathway probabilities. For each of these sites, a spreader factor or a sponge factor was then calculated as the ratio of P_{out}/P_{in}. Greater spreader factors represent stronger spreaders and conversely, smaller sponge factors represent stronger sponges. For $EGFR^{m}$ NSCLC the brain was a sponge (factor of 0.864), while in $EGFR^{wt}$ NSCLC the brain was a spreader (factor of 1.041). For both cases though, the adrenal gland was a sponge (factors of 0.720 for mutated and 0.235 for wild type).

Discussion

The classic view of metastatic progression, based on Paget's 'seed-and-soil' hypothesis, describes cancer spread in a unidirectional manner from primary tumor to distant metastatic sites [30]. However, this view has been challenged by multiple studies which suggest that metastatic spread can be a multidirectional process, whereby circulating tumor cells, or 'seeds', move in a number of ways: (i) seeds from the primary tumor re-enter the primary (primary self-seeding), (ii) seeds from metastatic sites re-enter the primary (primary re-seeding), or (iii) seeds from metastases re-enter metastatic sites (metastasis re-seeding) [27, 31, 32].

While other models have been used to predict clinical outcomes in lung cancer and other malignancies, most of these models are primarily dependent on variables collected at a single time point [33–35], and do not consider the dynamic nature of cancer as a process. In contrast, Markov modeling can be used to track cancer progression in a longitudinal manner over each patient's lifetime, while also tracking multiple events (e.g. development of metastatic sites) simultaneously. As such, this approach is more representative of the multidirectional spread of cancer, whereby the direc-

Table 2. Probabilities of Common Pathways for $EGFR^{m}$ and $EGFR^{wt}$ NSCLC.

Path	$EGFR^{m}$ (%)	$EGFR^{wt}$ (%)	% Diff (%)
Primary → Brain	12.9	11.1	1.8
Primary → Bone	8.1	3.0	5.1
Primary → Liver	11.3	15.2	3.9
Primary → Lung	56.5	52.5	4.0
Primary → LN (distant)	4.8	5.0	0.2
Primary → Adrenal	1.6	2.0	0.4
Primary → Bone → Lung	3.2	1.0	2.2
Primary → Bone → Brain	0.0	0.0	0.0
Primary → Bone → Liver	3.2	1.0	2.2
Primary → Lung → Brain	16.1	10.1	6.0
Primary → Lung → Bone	6.5	16.2	9.7
Primary → Lung → Liver	4.8	1.0	3.8
Primary → Lung → LN (distant)	3.2	8.1	4.9
Primary → Lung → Adrenal	1.6	3.0	1.4
Primary → Liver → Lung	8.1	9.1	1.0
Primary → Liver → Brain	1.6	2.0	0.4
Primary → Liver → Bone	1.6	1.0	0.6
Primary → Brain → Lung	3.2	2.0	1.2
Primary → Brain → Bone	3.2	4.0	0.8
Primary → LN (distant) → Lung	1.6	1.0	0.6
Primary → LN (distant) → Liver	1.6	0.0	1.6
Primary → LN (distant) → Bone	1.6	1.0	0.6
Primary → Bone → Lung → Brain	1.6	0.0	1.6
Primary → Liver → Lung → Brain	4.8	0.0	4.8
Primary → Liver → Lung → Bone → Brain	1.6	0.0	1.6
Primary → Brain → Bone → Lung → Brain	1.6	0.0	1.6
Primary → Lung → Chest Wall → Bone → Brain	1.6	0.0	1.6

tion in which seeds travel is independent of their past directions.

Newton *et al* [27] used Markov mathematical modeling to retrospectively analyze an autopsy database of lung cancer patients and their patterns of metastatic spread. Their results support the notion that lung cancer progression is likely a multidirectional process, as opposed to a unidirectional process. Their study also validated entropy as a metric for quantifying complexity in metastatic spread of cancer based on the dynamic predictability of cancer's progression [32]. However, there are notable differences with our study, as their database did not differentiate small cell from non-small cell lung cancer, nor did it distinguish between molecular subtypes, such as $EGFR^{m}$ and $EGFR^{wt}$ tumors. Furthermore, this data set established adrenal glands and kidneys as key spreaders, while regional lymph nodes, liver and bone were identified as key sponges for metastatic lung cancer [31]. In contrast, our results identified the bone, liver and lymph nodes as spreaders, and the adrenal glands as sponges. Our results may indicate the impact of systemic therapy, given that the earlier study included patients who were treated with surgery alone.

We employed Markov mathematical modeling in a database of actively treated NSCLC patients, and in doing so, found notable differences between $EGFR^{m}$ and $EGFR^{wt}$ NSCLC. First, our analysis identified the brain as an important sponge in $EGFR^{m}$ lung cancer; this adds to the already existing evidence of increased brain metastases in this subtype of lung cancer. Second, our Markov models identified a high probability of preferential spread of $EGFR^{m}$ lung cancer from lung primary to lung metastasis and then to brain metastasis. It should be noted that one limitation of our model is the small population of $EGFR^{m}$ and $EGFR^{wt}$ patients. As a result, we are unable to perform robust, quantitative statistics between the two, but instead offer up a highly detailed, qualitative assessment of the differences between these two groups. Larger datasets will allow for the creation of more accurate models, including the possibility of refining further differences between different genotype specific populations, such as ALK or ROS1 rearranged populations.

While prior studies have described the incidence of brain metastases in association with other metastatic sites among $EGFR^{m}$ lung cancer [9, 12, 23, 36], to our knowledge, this is the first study that describes a spatiotemporal progression from lung metastases to brain metastases in this population. Our patients with $EGFR^{m}$ NSCLC were significantly more likely to be treated with EGFR targeted therapy ($p < 0.0001$), so we cannot rule out the possibility that anatomic differences in progres-

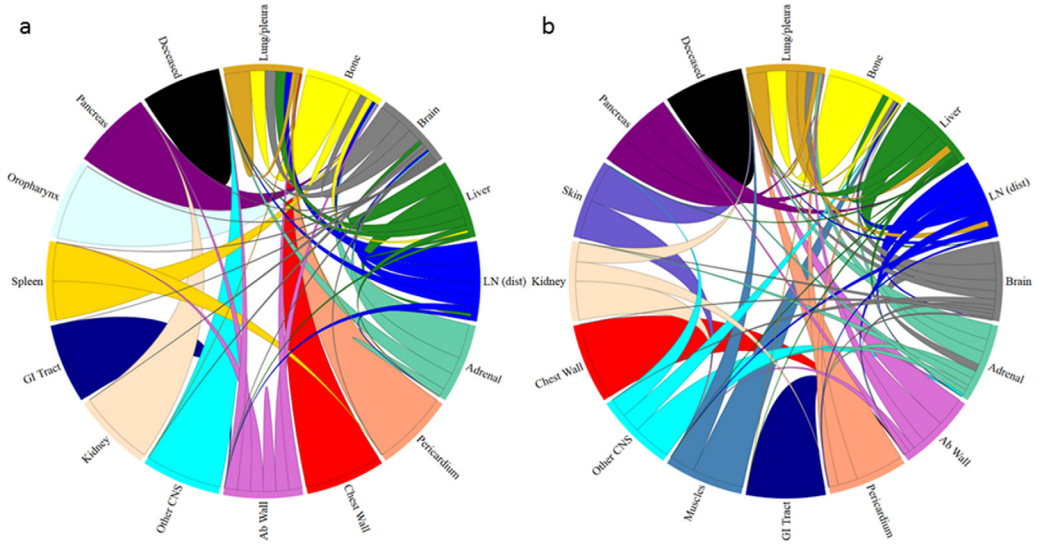

Figure 4. Markov chain network diagrams for (a) EGFR^{m} and (b) EGFR^{wt} lung cancer shown as circular chord diagrams with primary located at the 12:00 position. Metastatic sites are ordered clockwise from the primary in decreasing transition probability. Chord widths at their respective starting locations represent one-step transition probabilities between two sites.

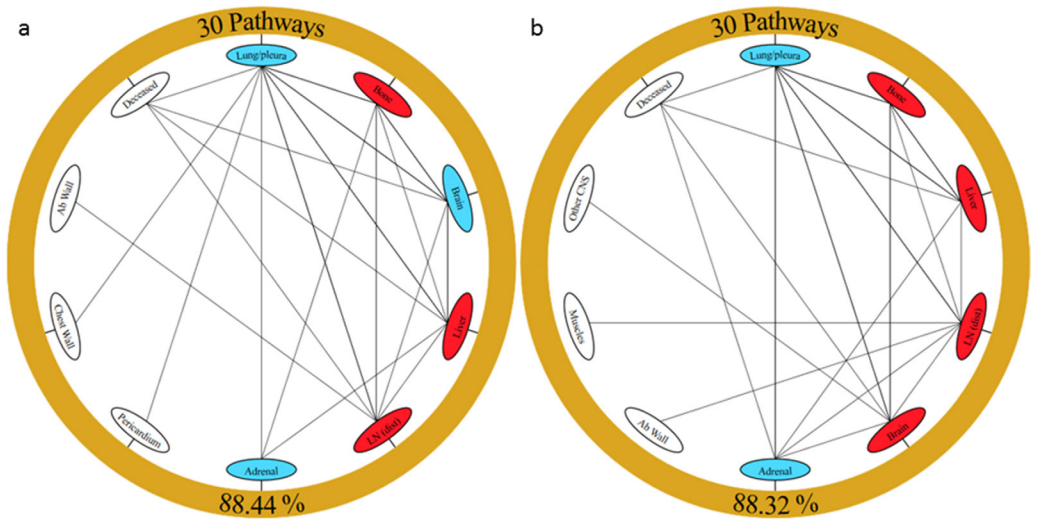

Figure 5. Reduced Markov diagrams showing the top 30 two-step pathways emanating from primary lung cancer (outer golden ring) for (a) EGFR^{m} and (b) EGFR^{wt}. The bottom value indicates the percentage of all two-step pathways that the figure represents. Nodes are classified as a 'spreader' (red) or 'sponge' (blue) based on the ratio of their outgoing and incoming probabilities. Two-step probabilities as well as P_{in} and P_{out} values can be found under supplemental figures (stacks.iop.org/CSPO/3/035002/mmedia).

sion are due to the impact of EGFR targeting drugs, rather than the EGFR mutation alone. The underlying biology that drives the linkage between lung metastasis and brain metastasis in EGFR^{m} NSCLC is a topic for future research with clinical implications. One prospective strategy may be to target this pathway of progression (e.g. radiation therapy to treat lung metastases) in the aim of hindering the development of brain metastases in EGFR^{m} NSCLC patients with existing lung metastases.

Although EGFR^{m} NSCLC patients have more brain metastases, they also have longer survival (see figures 1 and 2) [37–39]. This may be indicative of improved treatment of metastatic brain disease, including EGFR targeting agents such as gefitinib and erlotinib, which have shown response rates of up to 60–80% in EGFR^{m} brain metastases [40–43]. Novel EGFR targeting agents with even greater central nervous system (CNS) penetration are currently in development [44–46]. These therapies may also have a critical role for patients with EGFR^{m} pulmonary metastases, given the potential link with brain metastases that we have described. In our study, approximately 80% of EGFR^{m} patients received EGFR targeting agents, compared to only 20% of EGFR^{wt} patients, so we cannot discount the impact that these agents may have had in dictating anatomic progression of disease.

Current guidelines for NSCLC, such as those from the National Cancer Comprehensive Network (NCCN) [47], do not differentiate between EGFR^{m} and EGFR^{wt} patients with respect to the frequency and timing of brain imaging, yet brain metastases are a significant

cause of mortality and morbidity in the EGFR^{m} NSCLC population. If the presence of EGFR mutations, particularly in the setting of multifocal and/or progressive lung disease, portends increased risk for brain metastases, these patients may benefit from intensified CNS-specific imaging. Multi-modality strategies to treat limited metastatic disease and oligometastases have shown the potential to improve survival in advanced disease [48, 49], and may directly impact the biology of EGFR^{m} lung cancer when combined with targeted therapy [50].

Our results also showed a trend towards increased bone metastases in the EGFR^{wt} population, but without a specific anatomic pathway. NCCN guidelines do not recommend bone-targeted imaging in the absence of clinical symptoms [47], and asymptomatic bone metastases can still be missed [51, 52]. Given that bone-specific imaging and earlier consideration of bone-targeting agents (i.e. zoledronic acid) for affected patients may lead to decreased skeletal-related events and improved quality of life [53], the role of EGFR mutational status in bone metastases should be further investigated.

Patients with EGFR^{m} lung cancer and isolated progression of bone metastases appear to have better outcomes when treated with EGFR based therapy when compared to those with systemic progression [54, 55], but whether these differences are due to the EGFR mutation itself, or the effects of EGFR inhibition is unknown.

In conclusion, we utilized Markov modeling to characterize the progression of EGFR^{m} lung cancer from lung primary to lung metastasis and then to brain metastasis. Our findings indicate that the molecular and anatomical characterization of metastatic cancer are inherently connected. Further investigation is needed to delineate the underlying mechanism of these anatomic differences in metastatic progression, which may have predictive and prognostic utility in the management of personalized lung cancer. While there are currently no standard tools for predicting metastatic spread, we anticipate that Markov modeling may provide a vehicle for driving this approach forward in personalized lung cancer care.

Disclosures

The project described was supported in part by award number P30CA014089 from the National Cancer Institute. Otherwise, the listed authors have no other affiliations or involvement with any financial or non-financial interests to report.

ORCID

Gino K. In https://orcid.org/0000-0002-7060-5123

References

[1] Mok T S *et al* 2009 Gefitinib or carboplatin-paclitaxel in pulmonary adenocarcinomz *New Engl. J. Med.* **361** 947–57
[2] Shaw A T *et al* 2013 Crizotinib versus chemotherapy in advanced ALK-positive lung cancer *New Engl. J. Med.* **368** 2385–94
[3] Bergethon K *et al* 2012 ROS1 rearrangements define a unique molecular class of lung cancers *J. Clin. Oncol.* **30** 863–70
[4] Doebele R C *et al* 2012 Oncogene status predicts patterns of metastatic spread in treatment-naive nonsmall cell lung cancer *Cancer* **118** 4502–11
[5] Enomoto Y, Takada K, Hagiwara E and Kojima E 2013 Distinct features of distant metastasis and lymph node stage in lung adenocarcinoma patients with epidermal growth factor receptor gene mutations *Respir. Investig.* **51** 153–7
[6] Hendriks L E *et al* 2014 EGFR mutated non-small cell lung cancer patients: more prone to development of bone and brain metastases? *Lung Cancer* **84** 86–91
[7] Rangachari D *et al* 2015 Brain metastases in patients with EGFR-mutated or ALK-rearranged non-small-cell lung cancers *Lung Cancer* **88** 108–11
[8] Tseng C H *et al* 2016 EGFR mutation and lobar location of lung adenocarcinoma *Carcinogenesis* **37** 157–62
[9] Tanaka K *et al* 2015 EGFR Mutation impact on definitive concurrent chemoradiation therapy for inoperable stage III adenocarcinoma *J. Thorac Oncol.* **10** 1720–5
[10] Yagishita S *et al* 2015 Epidermal growth factor receptor mutation is associated with longer local control after definitive chemoradiotherapy in patients with stage III nonsquamous non-small-cell lung cancer *Int. J. Radiat. Oncol. Biol. Phys.* **91** 140–8
[11] Akamatsu H *et al* 2014 The impact of clinical outcomes according to EGFR mutation status in patients with locally advanced lung adenocarcinoma who recieved concurrent chemoradiotherapy *Am. J. Clin. Oncol.* **37** 144–7
[12] Guan J *et al* 2016 EGFR mutations are associated with higher incidence of distant metastases and smaller tumor size in patients with non-small-cell lung cancer based on PET/CT scan *Med. Oncol.* **33** 1
[13] Hasegawa M, Sakai F, Ishikawa R, Kimura F, Ishida H and Kobayashi K 2016 CT features of epidermal growth factor receptor-mutated adenocarcinoma of the lung: comparison with nonmutated adenocarcinoma *J. Thorac Oncol.* **11** 819–26
[14] Tsao A S *et al* 2006 Clinicopathologic characteristics of the EGFR gene mutation in non-small cell lung cancer *J. Thorac Oncol.* **1** 231–9
[15] Park J H *et al* 2013 Tumor burden is predictive of survival in patients with non-small-cell lung cancer and with activating epidermal growth factor receptor mutations who receive gefitinib *Clin. Lung Cancer* **14** 383–9
[16] Fujimoto D *et al* 2014 Features and prognostic impact of distant metastasis in patients with stage IV lung adenocarcinoma harboring EGFR mutations: importance of bone metastasis *Clin. Exp. Metastasis* **31** 543–51
[17] Shin D Y *et al* 2016 Epidermal growth factor receptor mutations and brain metastasis in patients with nonadenocarcinoma of the lung *J. Cancer Res. Ther.* **12** 318–22
[18] Hsu F, De Caluwe A, Anderson D, Nichol A, Toriumi T and Ho C 2016 EGFR mutation status on brain metastases from non-small cell lung cancer *Lung Cancer* **96** 101–7
[19] Wu K L *et al* 2015 Liver metastasis predicts poorer prognosis in stage IV lung adenocarcinoma patients receiving first-line gefitinib *Lung Cancer* **88** 187–94
[20] Sekine A *et al* 2012 Metastatic brain tumors from non-small cell lung cancer with EGFR mutations: distinguishing influence of exon 19 deletion on radiographic features *Lung Cancer* **77** 64–9
[21] Iuchi T *et al* 2015 Frequency of brain metastases in non-small-cell lung cancer, and their association with epidermal growth factor receptor mutations *Int. J. Clin. Oncol.* **20** 674–9
[22] Shin D Y, Na I I, Kim C H, Park S, Baek H and Yang S H 2014 EGFR mutation and brain metastasis in pulmonary adenocarcinomas *J. Thorac Oncol.* **9** 195–99
[23] Stanic K, Zwitter M, Hitij N T, Kern I, Sadikov A and Cufer T 2014 Brain metastases in lung adenocarcinoma: impact of EGFR mutation status on incidence and survival *Radiol. Oncol.* **48** 173–83
[24] Eichler A F *et al* 2010 EGFR mutation status and survival after diagnosis of brain metastasis in nonsmall cell lung cancer *Neurol. Oncol.* **12** 1193–9

[25] Heon S *et al* 2010 Development of central nervous system metastases in patients with advanced non-small cell lung cancer and somatic EGFR mutations treated with gefitinib or erlotinib *Clin. Cancer Res.* **16** 5873–82
[26] Sekine A *et al* 2014 Prognostic factors for brain metastases from non-small cell lung cancer with EGFR mutation: influence of stable extracranial disease and erlotinib therapy *Med. Oncol.* **31** 228
[27] Newton P K *et al* 2013 Spreaders and sponges define metastasis in lung cancer: a Markov chain Monte Carlo mathematical model *Cancer Res.* **73** 2760–9
[28] Sonnenberg F A and Beck J R 1993 Markov models in medical decision making: a practical guide *Med. Decis. Making* **13** 322–38
[29] Eisenhauer E A *et al* 2009 New response evaluation criteria in solid tumours: revised RECIST guideline (version 1.1) *Eur. J. Cancer* **45** 228–47
[30] Paget S 1989 The distribution of secondary growths in cancer of the breast 1889 *Cancer Metastasis Rev.* **8** 98–101
[31] Bazhenova L, Newton P, Mason J, Bethel K, Nieva J and Kuhn P 2014 Adrenal metastases in lung cancer: clinical implications of a mathematical model *J. Thorac Oncol.* **9** 442–6
[32] Newton P K *et al* 2014 Entropy, complexity, and Markov diagrams for random walk cancer models *Sci. Rep.* **4** 7558
[33] Genre L *et al* 2017 External validation of a published nomogram for prediction of brain metastasis in patients with extra-cerebral metastatic breast cancer and risk regression analysis *Eur. J. Cancer* **72** 200–9
[34] Kohne C H *et al* 2002 Clinical determinants of survival in patients with 5-fluorouracil-based treatment for metastatic colorectal cancer: results of a multivariate analysis of 3825 patients *Ann. Oncol.* **13** 308–17
[35] Shafazand S and Gould M K 2006 A clinical prediction rule to estimate the probability of mediastinal metastasis in patients with non-small cell lung cancer *J. Thorac. Oncol.* **1** 953–9
[36] Ng D Z *et al* 2016 139PD: lifetime incidence of brain metastases (BM) in EGFR-mutant (M+) lung cancer treated with first-line EGFR TKIs *J. Thorac Oncol.* **11** S117
[37] Inoue A *et al* 2013 Updated overall survival results from a randomized phase III trial comparing gefitinib with carboplatin-paclitaxel for chemo-naive non-small cell lung cancer with sensitive EGFR gene mutations (NEJ002) *Ann. Oncol.* **24** 54–9
[38] Wu Y L *et al* 2015 First-line erlotinib versus gemcitabine/cisplatin in patients with advanced EGFR mutation-positive non-small-cell lung cancer: analyses from the phase III, randomized, open-label, ENSURE study *Ann. Oncol.* **26** 1883–9
[39] Zhou C *et al* 2015 Final overall survival results from a randomised, phase III study of erlotinib versus chemotherapy as first-line treatment of EGFR mutation-positive advanced non-small-cell lung cancer (OPTIMAL, CTONG-0802) *Ann. Oncol.* **26** 1877–83
[40] Porta R *et al* 2011 Brain metastases from lung cancer responding to erlotinib: the importance of EGFR mutation *Eur. Respir. J.* **37** 624–31
[41] Kim J E *et al* 2009 Epidermal growth factor receptor tyrosine kinase inhibitors as a first-line therapy for never-smokers with adenocarcinoma of the lung having asymptomatic synchronous brain metastasis *Lung Cancer* **65** 351–4
[42] Ma S, Xu Y, Deng Q and Yu X 2009 Treatment of brain metastasis from non-small cell lung cancer with whole brain radiotherapy and Gefitinib in a Chinese population *Lung Cancer* **65** 198–203
[43] Park S J *et al* 2012 Efficacy of epidermal growth factor receptor tyrosine kinase inhibitors for brain metastasis in non-small cell lung cancer patients harboring either exon 19 or 21 mutation *Lung Cancer* **77** 556–60
[44] Ballard P *et al* 2016 Preclinical Comparison of osimertinib with other EGFR-TKIs in EGFR-Mutant NSCLC brain metastases models, and early evidence of clinical brain metastases activity *Clin. Cancer Res.* **22** 5130–40
[45] Ricciuti B *et al* 2016 Osimertinib (AZD9291) and CNS response in two radiotherapy-naive patients with EGFR-Mutant and T790M-Positive advanced non-small cell lung cancer *Clin. Drug Investig.* **36** 683–6
[46] Zeng Q *et al* 2015 Discovery and evaluation of clinical candidate AZD3759, a potent, oral active, central nervous system-penetrant, epidermal growth factor receptor tyrosine kinase inhibitor, preclinical comparison of osimertinib with other EGFR-TKIs in EGFR-Mutant NSCLC brain metastases models, and early evidence of clinical brain metastases activity *J. Med. Chem.* **58** 8200–15
[47] Ettinger D S *et al* 2017 Non-small cell lung cancer, version 5.2017, NCCN clinical practice guidelines in oncology *J. Natl Compr. Canc. Netw.* **15** 504–35
[48] Ashworth A B *et al* 2014 An individual patient data metaanalysis of outcomes and prognostic factors after treatment of oligometastatic non-small-cell lung cancer *Clin. Lung Cancer* **15** 346–55
[49] Hasselle M D *et al* 2012 Hypofractionated image-guided radiation therapy for patients with limited volume metastatic non-small cell lung cancer *J. Thorac Oncol.* **7** 376–81
[50] Iyengar P *et al* 2014 Phase II trial of stereotactic body radiation therapy combined with erlotinib for patients with limited but progressive metastatic non-small-cell lung cancer *J. Clin Oncol.* **32** 3824–30
[51] Erturan S, Yaman M, Aydin G, Uzel I, Musellim B and Kaynak K 2005 The role of whole-body bone scanning and clinical factors in detecting bone metastases in patients with non-small cell lung cancer *Chest* **127** 449–54
[52] Iordanidou L *et al* 2006 Is there a role of whole body bone scan in early stages of non small cell lung cancer patients *J. Buon.* **11** 491–7
[53] Rosen L S *et al* 2004 Long-term efficacy and safety of zoledronic acid in the treatment of skeletal metastases in patients with nonsmall cell lung carcinoma and other solid tumors: a randomized, phase III, double-blind, placebo-controlled trial *Cancer* **100** 2613–21
[54] Hong S H *et al* 2016 Clinical characteristics and continued epidermal growth factor receptor tyrosine kinase inhibitor administration in EGFR-mutated non-small cell lung cancer with skeletal metastasis *Cancer Res. Treat.* **48** 1110–9
[55] Hwang J A *et al* 2016 Clinical implications of isolated bone failure without systemic disease progression during EGFR-TKI treatment *Clin. Lung Cancer* **17** 573–80.e571